Fixed lines in a non-Hermitian Kitaev chain with spatially balanced pairing processes

Y. B. Shi and Z. Song*

School of Physics, Nankai University, Tianjin 300071, China

(Received 30 April 2023; revised 30 July 2023; accepted 6 September 2023; published 15 September 2023)

Exact solutions for non-Hermitian quantum many-body systems are rare but may provide valuable insights into the interplay between Hermitian and non-Hermitian components. We report our investigation of a non-Hermitian variant of a *p*-wave Kitaev chain by introducing staggered imbalanced pair creation and annihilation terms. We find that there exist fixed lines in the phase diagram, at which the ground state remains unchanged in the presence of a non-Hermitian term under the periodic boundary condition for a finite system. This allows the constancy of the topological index in the process of varying the balance strength at arbitrary rate, exhibiting the robustness of the topology for the non-Hermitian Kitaev chain under time-dependent perturbations. The underlying mechanism is investigated through the equivalent quantum spin system obtained by the Jordan-Wigner transformation for infinite chain. In addition, the exact solution shows that a resonant non-Hermitian impurity can induce a pair of zero modes in the corresponding Majorana lattice, which asymptotically approach the edge modes in the thermodynamic limit, manifesting the bulk-boundary correspondence. Numerical simulation is performed for the quench dynamics for the systems with slight deviation from the fixed lines to show the stability region in time. This work reveals the interplay between the pair creation and annihilation pairing processes.

DOI: 10.1103/PhysRevB.108.125121

I. INTRODUCTION

The exact solution of a model Hamiltonian plays an important role in physics and sometimes may open the door to the exploration of new frontiers in physics. One recent example is the discovery of the solution for a non-Hermitian harmonic system, which is a starting point of PT-symmetric quantum mechanics [1–4]. In traditional quantum mechanics, the fundamental postulate of the Hermiticity of the Hamiltonian ensures the reality of the spectrum and the unitary dynamics for a closed quantum system [5]. In general, any Hermitian Hamiltonian can also be decomposed into two non-Hermitian sub-Hamiltonians that are Hermitian conjugates of each other. Intuitively, the reality of the spectrum is rooted in the balance of the actions of the two non-Hermitian sub-Hamiltonians. In this sense, the Hermiticity is not necessary for the balance, since the balance can be established across a distance by a pseudo-Hermitian Hamiltonian [6–11], for instance, a simple gain-loss-balanced system in Refs. [12–14]. However, exact solutions for non-Hermitian quantum many-body systems are rare but provide valuable insights into the physics of quantum matter. In this work, we present a much more compelling example to demonstrate the balance in a non-Hermitian quantum many-body system and reveal the interplay between Hermitian and non-Hermitian components.

We study a non-Hermitian variant of a *p*-wave Kitaev chain [15] by introducing staggered imbalanced pair creation and annihilation terms. The staggered arrangement provides the balance between two neighboring dimers. In most works, the balanced terms usually arise from single-particle processes, such as hopping or on-site potential terms. In previous work [16], it has been shown that a non-Hermitian term for the pairing process can alter the phase diagram in the ground state. In this work, the non-Hermitian components are extended. Based on the exact solutions, we find that there exists a family of lines, at which the ground state of the Hamiltonian remains unchanged in the presence of a non-Hermitian term under the periodic boundary condition for a finite system. The ground state is only determined by the intercept of a given line, referred to as a fixed line.

It is well known that the topological superconducting phase in the original Kitaev model has been demonstrated by the winding number of the Majorana lattice and unpaired Majorana modes exponentially localized at the ends of open Kitaev chains [17–19]. For the present model, our result is the constancy of the winding number in the process of varying the balance strength at an arbitrary rate, exhibiting the robustness of the topology for a non-Hermitian Kitaev chain under time-dependent perturbations. In addition, the exact solution shows that a resonant non-Hermitian impurity can induce a pair of zero modes in the corresponding Majorana lattice, which asymptotically approach the edge modes in the thermodynamic limit, manifesting the bulk-boundary correspondence. The underlying mechanism is investigated through the equivalent quantum spin system [20] obtained by the Jordan-Wigner transformation [21] for finite chains. Starting from the explicit ground states of the open spin chain, we elaborate that the non-Hermitian terms have no energy contribution in the bulk and show how the stringlike boundary term hybridizes two ferromagnetic states. We also investigate the stability region in time for systems with a slight deviation from the fixed lines by performing numerical simulation of quench dynamics. This work reveals the interplay between the

*songtc@nankai.edu.cn

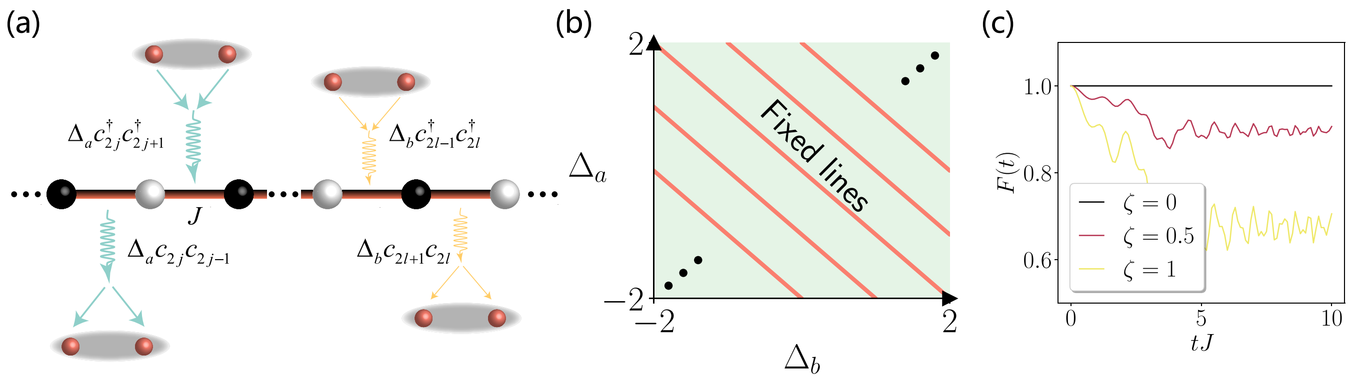

FIG. 1. (a) Schematic of a 1D Kitaev model for spinless fermion with non-Hermitian imbalanced pair terms. It consists of two sublattices A and B in black and white, respectively. Here, J is the hopping strength between two adjacent sites. Δ_a is the strength of the p-wave pair creation (annihilation) on the odd (even) dimer, while Δ_b is the strength of the p-wave pair annihilation (creation) on the even (odd) dimer. (b) Schematic illustration of fixed lines. The fixed lines are a family of parallel lines with slope -1 in the Δ_a-Δ_b plane. The Hamiltonians with parameters at each line share the same ground state with the same energy, which are determined only by the intercepts of the line. The intercepts of the five representative lines are -2, -1, 0, 1, and 2. (c) Plot of the fidelity for the dynamic process in the system with different time-dependent parameters in Eq. (17). It indicates that when the time-dependent parameters only move along a fixed line, the fidelity is always equal to 1.

pair creation and annihilation pairing processes at different locations.

This paper is organized as follows. In Sec. II, we describe the model Hamiltonian and present the exact solution. In Sec. III, we study the corresponding Majorana lattice to show the exact zero modes in the presence of an engineered impurity. In Sec. IV, we investigate our model in the spin representation. In Sec. V, we present the features of the dynamic behavior when the quench Hamiltonian deviates from the fixed lines. Finally, we give a summary and discussion in Sec. VI. Some details of derivations are placed in the Appendix.

II. MODEL AND FIXED LINES

We consider the following non-Hermitian fermionic Hamiltonian $H = H(\Delta_a, \Delta_b, \mu)$ on a lattice of length $2N$ (even N):

$$H = J\sum_{l=1}^{2N} c_l^\dagger c_{l+1} + \text{H.c.} + \mu \sum_{l=1}^{2N}(1-2n_l) + \sum_{j=1}^{N}(\Delta_a c_{2j}^\dagger c_{2j+1}^\dagger + \Delta_a c_{2j}c_{2j-1} + \Delta_b c_{2j+1}c_{2j} + \Delta_b c_{2j-1}^\dagger c_{2j}^\dagger), \quad (1)$$

where $c_l^\dagger$ (c_l) is a fermionic creation (annihilation) operator on site l, $n_l = c_l^\dagger c_l$, J is the tunneling rate, and real number Δ_a is the strength of the p-wave pair creation (annihilation) on the odd (even) dimer, while Δ_b the strength of the p-wave pair annihilation (creation) on the even (odd) dimer. μ is the chemical potential. The non-Hermitian Kitaev model is schematically illustrated in Fig. 1(a). For a closed chain, we define $c_{2N+1} = c_1$ and for an open chain, we set $c_{2N+1} = 0$. The Kitaev model is known to have a rich phase diagram in its Hermitian version, i.e., $H \rightarrow H + H^\dagger$, or $\Delta_a = \Delta_b$. In particular, in the nontrivial topological region, the ground state is twofold degenerate in the large N limit, which stems from the Majorana zero modes. In this work, we focus on what happens when $\Delta_a \neq \Delta_b$. To be more precise, we investigate the influence of the non-Hermitian terms on the topological phase and the edge modes of the corresponding Majorana lattice.

We introduce the Fourier transformations in two sublattices

$$\begin{pmatrix} c_{2j-1} \\ c_{2j} \end{pmatrix} = \frac{1}{\sqrt{N}}\sum_k e^{ikj}\begin{pmatrix} \alpha_k \\ \beta_k \end{pmatrix} \quad (2)$$

and, inversely, the spinless fermionic operators in k space α_k, β_k are

$$\begin{pmatrix} \alpha_k \\ \beta_k \end{pmatrix} = \frac{1}{\sqrt{N}}\sum_k e^{-ikj}\begin{pmatrix} c_{2j-1} \\ c_{2j} \end{pmatrix}, \quad (3)$$

where $j = 1, 2, \ldots, N$, $k = 2m\pi/N$, and $m = 0, 1, 2, \ldots, N-1$. The Hamiltonian with periodic boundary condition can be block diagonalized by this transformation due to its translational symmetry, i.e.,

$$H = \sum_{k\in[0,\pi]} H_k = H_0 + H_\pi + \sum_{k\in(0,\pi)} \psi_k^\dagger h_k \psi_k, \quad (4)$$

satisfying $[H_k, H_{k'}] = 0$, where the operator vector $\psi_k^\dagger = (\alpha_k^\dagger \quad \beta_k^\dagger \quad \alpha_{-k} \quad \beta_{-k})$, and the core matrix is expressed explicitly as

$$h_k = \begin{pmatrix} -2\mu & J(1+e^{-ik}) & 0 & \Delta_b - \Delta_a e^{-ik} \\ J(1+e^{ik}) & -2\mu & \Delta_a e^{ik} - \Delta_b & 0 \\ 0 & \Delta_b e^{-ik} - \Delta_a & 2\mu & -J(1+e^{-ik}) \\ \Delta_a - \Delta_b e^{ik} & 0 & -J(1+e^{ik}) & 2\mu \end{pmatrix}. \quad (5)$$

Here, H_0 and H_π have the form

$$H_0 = 2J\alpha_0^\dagger\beta_0 + 2J\beta_0^\dagger\alpha_0 + 2\mu(\alpha_0\alpha_0^\dagger - \beta_0^\dagger\beta_0) + (\Delta_b - \Delta_a)(\alpha_0^\dagger\beta_0^\dagger + \alpha_0\beta_0), \tag{6}$$

$$H_\pi = 2\mu(\alpha_\pi\alpha_\pi^\dagger - \beta_\pi^\dagger\beta_\pi) + (\Delta_b + \Delta_a)(\alpha_\pi^\dagger\beta_\pi^\dagger + \beta_\pi\alpha_\pi). \tag{7}$$

The eigenvalue ϵ_k and eigenvector $|\varphi_k\rangle$ of h_k, satisfying $h_k|\varphi_k\rangle = \epsilon_k|\varphi_k\rangle$, can be obtained analytically or numerically, which will be used for numerical simulation of quench dynamics.

In the following, we focus on the case with $\mu = 0$. The Hamiltonian H can be expressed in the diagonal form of the Hamiltonian

$$H = H_0 + H_\pi + \sum_{k\in(0,\pi)}\sum_{\rho\sigma}\varepsilon_{\rho\sigma}^k\overline{A}_{\rho\sigma}^k A_{\rho\sigma}^k, \tag{8}$$

where

$$\varepsilon_{\rho\sigma}^k = \rho\sqrt{\left(2J\cos\frac{k}{2}\right)^2 + (\Delta_a+\Delta_b)^2\sin^2\frac{k}{2}} + i\sigma(\Delta_a - \Delta_b)\cos\frac{k}{2} \tag{9}$$

and the form of $A_{\rho\sigma}^k$ is presented in the Appendix and is independent of the value of $(\Delta_a - \Delta_b)$, satisfying the canonical commutation relations

$$\{A_{\rho\sigma}^k, \overline{A}_{\rho'\sigma'}^{k'}\} = \delta_{kk'}\delta_{\rho\rho'}\delta_{\sigma\sigma'},$$
$$\{A_{\rho\sigma}^k, A_{\rho'\sigma'}^{k'}\} = \{\overline{A}_{\rho\sigma}^k, \overline{A}_{\rho'\sigma'}^{k'}\} = 0. \tag{10}$$

Then the ground state is

$$|\mathrm{G}\rangle = \frac{1}{2}(\alpha_\pi^\dagger\beta_\pi^\dagger + 1)(\alpha_0^\dagger - \beta_0^\dagger)|0\rangle \times \prod_{k\in(0,\pi)}\overline{A}_{-+}^k\overline{A}_{--}^k|\mathrm{Vac}\rangle \tag{11}$$

with ground state energy

$$E_\mathrm{g} = 2\sum_{k\in(0,\pi)}\mathrm{Re}\varepsilon_{-+}^k - (2J + \Delta_a + \Delta_b). \tag{12}$$

Here $|\mathrm{Vac}\rangle$ is the vacuum state of the set of operator $\{A_{\rho\sigma}^k\}$, i.e., $A_{\rho\sigma}^k|\mathrm{Vac}\rangle = 0$, while $|0\rangle$ is the vacuum state of the fermion operators. We find that $|\mathrm{G}\rangle$ and E_g are both independent of the strength of the non-Hermiticity $\Delta_a - \Delta_b$ along the zero-μ line in the phase diagram. To describe this phenomenon, we dub the lines with slope -1 in the Δ_a-Δ_b plane "fixed lines," which are clearly depicted in Fig. 1(b).

Based on the above analysis, one can consider a time-dependent Hamiltonian $H(t)$ with the constraint $d(\Delta_a + \Delta_b)/dt = 0$, but $d(\Delta_a - \Delta_b)/dt \neq 0$. Considering the fact that the ground state and the energy are independent of the value of $\Delta_a - \Delta_b$, when $d(\Delta_a + \Delta_b)/dt = 0$, based on the fact

$$H(t)|\mathrm{G}\rangle = H(t')|\mathrm{G}\rangle = \varepsilon_g|\mathrm{G}\rangle \tag{13}$$

or

$$\exp[-iH(n\tau)\tau]|\mathrm{G}\rangle = e^{i\varepsilon_g\tau}|\mathrm{G}\rangle, \tag{14}$$

we have

$$|\Phi(t)\rangle = \mathcal{T}\exp\left[-i\int_0^t H(t)dt\right]|\mathrm{G}\rangle = \lim_{\tau\to 0}\mathcal{T}\prod_{n=1}^{N}\exp(-i\varepsilon_g\tau)|\,\mathrm{G}\rangle = e^{i\phi}|\mathrm{G}\rangle, \tag{15}$$

where $\mathcal{T}$ is the time-order operator and ϕ is an overall phase. The Hamiltonian $H(t)$ is the Hamiltonian shown in Eq. (1) with time-dependent parameters $\Delta_a(t) - \Delta_b(t)$. In Fig. 1(c), we provide the fidelity

$$F(t) = |\langle\Phi(0)|\Phi(t)\rangle|^2, \tag{16}$$

for a concrete system with

$$\Delta_a = 1 + \sin t^2, \quad \Delta_b = 1 - \sin(t^2 + \zeta), \tag{17}$$

by taking different $\zeta = 0$, 0.5, 1. The plot shows that the fidelity is always equal to 1 at the fixed line. This allows for the constancy of the winding number extracted from the ground state in the process of varying the balance strength at an arbitrary rate $d(\Delta_a - \Delta_b)/dt$, exhibiting the robustness of the topology for the non-Hermitian Kitaev chain under time-dependent perturbations $d(\Delta_a - \Delta_b)/dt$ [16]. However, the situation may change under the open condition, which will be investigated in the following section.

III. MAJORANA ZERO MODES

As mentioned above, it has been appreciated previously that bulk-boundary correspondence holds in the Hermitian Kitaev model. The analysis in the last section shows that the ground state remains unchanged at the fixed lines, maintaining the topology feature in the presence of non-Hermitian terms. However, the periodic condition plays an important role in such a conclusion, which will also be demonstrated in the next section in the context of the quantum spin model. In other words, the non-Hermitian terms should break the constancy of the ground state when an open boundary condition is taken. A natural question is whether edge modes still exist for the opened Majorana lattice in the presence of non-Hermitian terms.

We begin with a defected Kitaev system by introducing a resonant impurity located at a dimer across two sites $(1, 2N)$. The Hamiltonians read

$$H_\mathrm{D} = H - \lambda M,$$
$$M = \Delta_a c_{2N}^\dagger c_1^\dagger + \Delta_b c_1 c_{2N} + Jc_{2N}^\dagger c_1 + Jc_1^\dagger c_{2N}, \tag{18}$$

where λ controls the strength of the impurity and $\lambda = 1$ indicates the open chain. We introduce Majorana fermion operators

$$a_j = c_j^\dagger + c_j, \quad b_j = -i(c_j^\dagger - c_j), \tag{19}$$

which satisfy the relations

$$\{a_j, a_{j'}\} = 2\delta_{j,j'}, \quad \{b_j, b_{j'}\} = 2\delta_{j,j'},$$
$$\{a_j, b_{j'}\} = 0. \tag{20}$$

The inverse transformation is

$$c_j^\dagger = \tfrac{1}{2}(a_j + ib_j), \quad c_j = \tfrac{1}{2}(a_j - ib_j). \tag{21}$$

The Majorana representation of the Hamiltonian has the form

$$H_\mathrm{D} = \sum_{l=1}^{N}\left[\kappa_+\left(ib_{2j}a_{2j+1} + ib_{2j-1}a_{2j}\right) + \kappa_-(ib_{2j}a_{2j-1} + ib_{2j+1}a_{2j}) + \frac{\Delta_a - \Delta_b}{4}(a_{2j}a_{2j+1} + b_{2j+1}b_{2j} + a_{2j}a_{2j-1} + b_{2j-1}b_{2j})\right]$$
$$- \lambda\left[\kappa_+ ib_{2N}a_1 + \kappa_- ib_1 a_{2N} + \frac{\Delta_a - \Delta_b}{4}(a_{2N}a_1 + b_1 b_{2N})\right], \tag{22}$$

with $\kappa_\pm = [2J \pm (\Delta_a + \Delta_b)]/4$. We write down the Hamiltonian in the basis $\varphi^\dagger = (-ia_1, b_1, -ia_2, b_2, -ia_3, b_3, \dots)$ in the form

$$H_\mathrm{D} = \varphi^\dagger h_\mathrm{D} \varphi, \tag{23}$$

where h_D represents a $4N \times 4N$ matrix. Here, the matrix h_D can be explicitly written as

$$h_\mathrm{D} = \frac{\Delta_a - \Delta_b}{8}\sum_{j=1}^{N}(|2j, A\rangle\langle 2j+1, A| + |2j+1, B\rangle\langle 2j, B| + |2j, A\rangle\langle 2j-1, A| + |2j-1, B\rangle\langle 2j, B|) - \mathrm{H.c.}$$
$$+ \sum_{l=1}^{2N}\left(\frac{\kappa_+}{2}|l, B\rangle\langle l+1, A| + \frac{\kappa_-}{2}|l+1, B\rangle\langle l, A| + \mathrm{H.c.}\right)$$
$$- \lambda\left[\frac{\kappa_+}{2}(|2N, B\rangle\langle 1, A| + \mathrm{H.c.}) + \frac{\kappa_-}{2}(|1, B\rangle\langle 2N, A| + \mathrm{H.c.}) + \frac{\Delta_a - \Delta_b}{8}(|2N, A\rangle\langle 1, A| + |1, B\rangle\langle 2N, B| - \mathrm{H.c.})\right]. \tag{24}$$

In Fig. 2 the geometry of the lattice h_D is illustrated. We start with the perfect case with $\lambda = 0$ and the matrix describes a uniform ladder with unequal hopping strength under the periodic boundary condition. The spectrum of the matrix can be easily obtained as

$$\mathcal{E}_K = \pm\frac{1}{4}\sqrt{(2J)^2\cos^2 K + (\Delta_a + \Delta_b)^2\sin^2 K}$$
$$\pm i\frac{(\Delta_a - \Delta_b)}{4}\cos K, \tag{25}$$

which is one-quarter of $\varepsilon_{\rho\sigma}^k$ in Eq. (9), where the wave vector $K = m\pi/N$, $m = 0, 1, 2, \dots, N-1$. When $\mathcal{E}_K$ is considered as the energy band of a non-Hermitian system, i.e., a tight-binding ladder, the half filled ground state energy can be obtained as

$$E_\mathrm{g} = -\frac{N}{\pi}\max(2J, \Delta_a + \Delta_b)\mathrm{E}(e), \tag{26}$$

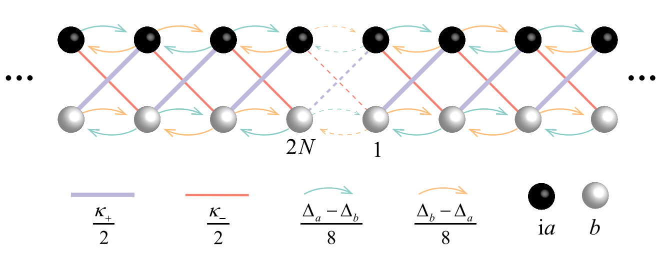

FIG. 2. Geometry for the Majorana lattice described in Eq. (24). The system consists of two sublattices, ia and b, indicated by black and white circles, respectively. The red and purple solid lines indicate the couplings between the sublattices. The yellow and green arrows are the unidirectional hopping. There is an engineered impurity, which is labeled as the dashed lines and arrows. The corresponding zero modes are plotted in Fig. 3.

which is obviously independent of $\Delta_a - \Delta_b$. Here function E means the complete elliptic integral of the second kind and e represents the eccentricity of the ellipse with width $2J$ and height $\Delta_a + \Delta_b$.

The translational symmetry is broken when we take $\lambda \neq 0$. Our goal is to find out the zero modes when taking the open boundary. To this end, we consider the cases with resonant conditions $\lambda = \lambda_+ = 1 - \gamma^{-N}$ and $\lambda_- = 1 - \gamma^N$, respectively. Under this condition, there always exist two zero modes for any given N. Importantly, it provides explicit expressions of the zero modes even in the finite N limit. The coefficient γ has the form

$$\gamma = \frac{|\Delta_a + \Delta_b|\sqrt{(\Delta_a - \Delta_b)^2 + 4J^2} - 2J^2 - \Delta_a^2 - \Delta_b^2}{2(J^2 - \Delta_a\Delta_b)}, \tag{27}$$

which determines the values of $\lambda = 1$ or ∞, in the large N limit. Accordingly, H_D describes an open ladder of $4N$ and $(4N-4)$ sites, respectively, when N turns to infinity. Straightforward derivations show the following exact results. There are a pair of zero modes

$$h_\mathrm{D}|\psi_\mathrm{L}\rangle = h_\mathrm{D}|\psi_\mathrm{R}\rangle = 0, \tag{28}$$

for arbitrary N, when taking $\lambda = \lambda_\pm$. Leaving aside the overall normalization, (i) for $\lambda = \lambda_-$, we have the explicit expression of zero modes

$$|\psi_\mathrm{L}\rangle = \sum_{j=1}^{2N}\gamma^{j-1}(|2j-1, A\rangle + \beta|2j-1, B\rangle),$$
$$|\psi_\mathrm{R}\rangle = \sum_{j=1}^{2N}\gamma^{N-j}(|2j, B\rangle + \beta|2j, A\rangle), \tag{29}$$

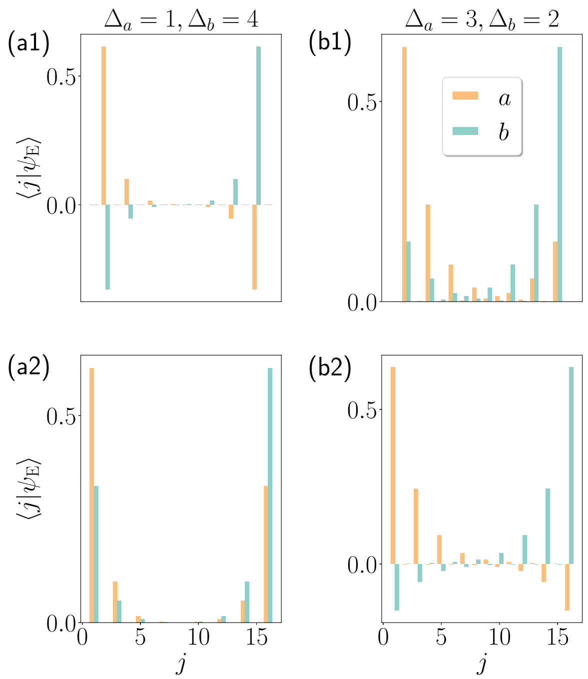

FIG. 3. Profiles of the zero modes from Eq. (31) for Majorana lattices in Fig. 2 with $N = 8$. The first row is the plot for the system with the condition $\lambda = \lambda_-$ and the second row with the condition $\lambda = \lambda_+$. The color bars indicate the amplitudes of two different sublattices. All four patterns exhibit evident skin effect.

while (ii) for $\lambda = \lambda_+$, we have

$$\begin{aligned}|\psi_{\rm R}\rangle &= \sum_{j=1}^{2N} \gamma^{N-j}(|2j-1, B\rangle - \beta|2j-1, A\rangle),\\ |\psi_{\rm L}\rangle &= \sum_{j=1}^{2N} \gamma^{j-1}(|2j, A\rangle - \beta|2j, B\rangle),\end{aligned} \tag{30}$$

where the coefficient is $\beta = [\sqrt{4J^2 + (\Delta_b - \Delta_a)^2} - 2J]/(\Delta_b - \Delta_a)$. The exact result is demonstrated by the plot of the profile of the normalized edge state

$$|\psi_{\rm E}\rangle = \frac{|\psi_{\rm R}\rangle}{\sqrt{2}||\psi_{\rm R}\rangle|} + \frac{|\psi_{\rm L}\rangle}{\sqrt{2}||\psi_{\rm L}\rangle|}, \tag{31}$$

in Fig. 3 for finite N. It is obvious that the zero modes are standard edge modes, demonstrating the bulk-edge correspondence at $\lambda = 1$ in the thermodynamic limit.

Compared to the ground state for a periodic boundary condition, the profiles of edge modes $|\psi_{\rm L,R}\rangle$ are now dependent on the value of $\Delta_a - \Delta_b$. This means that the non-Hermitian components have an effect on the eigenstates when the translational symmetry is broken. It may be because the balance between the staggered imbalanced pair creation and annihilation terms is broken. To understand how the non-Hermitian components cancel each other out, in the following section, we study the model in the spin representation.

IV. DISSIPATIONLESS FERROMAGNETIC ORDER

It has been noted that the Kitaev chain, a p-wave superconductor, can be mapped into a quantum spin XY model with a transverse field via a Jordan-Wigner transformation [21], replacing the spinless fermion creation and annihilation operators with spin flip operators. Accordingly, the present non-Hermitian Kitaev model should correspond to a non-Hermitian XY model. Intuitively, a spin model can provide a clear physical picture for understanding the balance of non-Hermitian terms from different locations. The non-Hermitian extensions for quantum spin XY model have been studied via several examples [22–24]. However, the non-Hermitian spin model mapped from a Kitaev model is slightly special. It possesses a subtle boundary term involving a string operator. In this section, we consider this problem based on the simplest case with $\Delta_a + \Delta_b = 2J$.

Introducing the Jordan Winger transformation

$$c_j = \prod_{i=1}^{j-1} \sigma_i^z \sigma_j^-, \quad c_j^\dagger = \prod_{i=1}^{j-1} \sigma_i^z \sigma_j^+, \tag{32}$$

the Kitaev Hamiltonian can be expressed as

$$H = JH_0 + \frac{i(\Delta_a - \Delta_b)}{4}\mathcal{H}, \tag{33}$$

where both terms

$$H_0 = -\sum_{l=1}^{2N-1} \sigma_l^x \sigma_{l+1}^x - \left(\prod_{i=2}^{2N-1} \sigma_i^z\right)\sigma_1^y \sigma_{2N}^y \tag{34}$$

and

$$\begin{aligned}\mathcal{H} = &\sum_{j=1}^{N} \left(\sigma_{2j-1}^x \sigma_{2j}^y + \sigma_{2j-1}^y \sigma_{2j}^x\right) - \sum_{j=1}^{N-1} \left(\sigma_{2j}^y \sigma_{2j+1}^x + \sigma_{2j}^x \sigma_{2j+1}^y\right)\\ &+ \left(\prod_{i=2}^{2N-1} \sigma_i^z\right)\left(\sigma_1^y \sigma_{2N}^x + \sigma_{2N}^y \sigma_1^x\right)\end{aligned} \tag{35}$$

are all Hermitian. We note that H_0 represents the simplest Ising model but with a subtle boundary condition $(\Pi_{i=2}^{2N-1}\sigma_i^z)\sigma_1^y\sigma_{2N}^y$, which contains a stringlike nonlocal operator $\Pi_{i=1}^{2N}\sigma_i^z$. The effect of the boundary condition has rarely been considered in previous investigations on the Ising model and is important in this work. It is well known that the GHZ states [25–27]

$$|{\rm GHZ}^\pm\rangle = \frac{1}{\sqrt{2}}\left(\prod_{i=1}^{2N}|\uparrow\rangle_i \pm \prod_{i=1}^{2N}|\downarrow\rangle_i\right) \tag{36}$$

are the ground state doublet of H_0 when the boundary condition is modified by taking $(\Pi_{i=2}^{2N-1}\sigma_i^z)\sigma_1^y\sigma_{2N}^y \longrightarrow \sigma_1^x\sigma_{2N}^x$ or $(\Pi_{i=2}^{2N-1}\sigma_i^z)\sigma_1^y\sigma_{2N}^y \longrightarrow 0$. Here the kets are defined as $\sigma_i^x|\uparrow\rangle_i = |\uparrow\rangle_i$ and $\sigma_i^x|\downarrow\rangle_i = -|\downarrow\rangle_i$. However, straightforward derivation shows that

$$H_0|{\rm GHZ}^\pm\rangle = (-2N + 1 \pm 1)|{\rm GHZ}^\pm\rangle, \tag{37}$$

which indicates that $|{\rm GHZ}^-\rangle$ is the ground state singlet of H_0. Remarkably, when $\mathcal{H}$ is taken into account, one can find the relation

$$\sigma_l^y(\sigma_{l-1}^x - \sigma_{l+1}^x)|{\rm GHZ}^\pm\rangle = 0, \tag{38}$$

for $l \in [2, 2N-1]$ in the bulk. It is clear that the non-Hermitian spin coupling terms from two neighboring dimers cancel each other out when they are applied to the bulk of the ferromagnetic state. Furthermore, applying $\mathcal{H}$ to the state $|\mathrm{GHZ}^{\pm}\rangle$, we have

$$\mathcal{H}|\mathrm{GHZ}^{\pm}\rangle = \left(\sigma_1^y\sigma_2^x + \sigma_{2N-1}^x\sigma_{2N}^y\right)|\mathrm{GHZ}^{\pm}\rangle + \left(\sigma_1^y\sigma_{2N}^x + \sigma_{2N}^y\sigma_1^x\right)\left(\prod_{i=2}^{2N-1}\sigma_i^z\right)|\mathrm{GHZ}^{\pm}\rangle, \quad (39)$$

i.e., the action of $\mathcal{H}$ on state $|\mathrm{GHZ}^{\pm}\rangle$ is only left at the boundary. Then we have

$$\mathcal{H}|\mathrm{GHZ}^{-}\rangle = 0, \quad (40)$$

due to the fact that

$$\left(\sigma_1^y\sigma_{2N}^x + \sigma_{2N}^y\sigma_1^x\right)\left(\prod_{i=2}^{2N-1}\sigma_i^z\right)|\mathrm{GHZ}^{\pm}\rangle = \left(\sigma_1^x\sigma_{2N}^y + \sigma_{2N}^x\sigma_1^y\right)(\pm)|\mathrm{GHZ}^{\pm}\rangle. \quad (41)$$

The above investigation has shown that $|\mathrm{GHZ}^{-}\rangle$ is still the ground state of H. The ground state wave function is independent of the value of $(\Delta_a - \Delta_b)$ which is in accord with the analysis in the last section. The underlying mechanism is that a pair of non-Hermitian terms from two neighboring dimers cancel each other out, leaving the GHZ states with perfect ferromagnetic order. For the other phases, $\Delta_a + \Delta_b \neq 2J$, next to the fixed line we mentioned in this section, there also exists a corresponding fixed line on which the ground state is the same as that of the corresponding Hermitian quantum XY model. The topological feature of the Hamiltonian with $\Delta_a \neq 0$, $\Delta_b = 0$ has been studied in Ref. [16]. In addition, the obtained result can be applied to other quantum spin systems. For example, when we consider a Heisenberg ring with an additional non-Hermitian term $i\sum_{j=1}^{N}(\sigma_{2j-1}^x\sigma_{2j}^y - \sigma_{2j}^y\sigma_{2j+1}^x)$, it is easy to find that the ferromagnetic states in the x direction remain unchanged. The ferromagnetic order does not dissipate in the presence of such non-Hermitian fluctuations.

V. STABILITY OF QUENCH DYNAMICS

In this section, we present the features of the dynamic behavior when the quench Hamiltonian deviates from the fixed lines by small nonzero μ. To be precise, in the following, we consider the numerical simulation of the quench process under the Hamiltonian

$$H_{\mathrm{pre}} = H(\Delta_a, \Delta_b, 0), \quad H_{\mathrm{pos}} = H(\Delta_a, \Delta_b, \mu), \quad (42)$$

where $H(\Delta_a, \Delta_b, \mu)$ is defined at the beginning in Eq. (1). To capture the effect of small μ on the dynamics, we introduce the concept of fidelity, which is a measure of the stability of the original quantum state under the perturbation. An initial quantum state $|\Phi(0)\rangle$ evolves during time t under postquench Hamiltonian H_{pos} reaching state $|\Phi(t)\rangle = e^{-iH_{\mathrm{pos}}t}|\Phi(0)\rangle$. The fidelity is defined as

$$F(t) = |\langle\Phi(0)|e^{-iH_{\mathrm{pos}}t}|\Phi(0)\rangle|^2. \quad (43)$$

In our study, the initial state is prepared as the ground state of H_{pre}, i.e., $|\Phi(0)\rangle = |\mathrm{G}\rangle$. Obviously, we always have $F(t) = 1$ when $H_{\mathrm{pre}} = H(\Delta_a, \Delta_b, 0)$ and $H_{\mathrm{pos}} = H(\Delta_a', \Delta_b', 0)$ with $\Delta_a + \Delta_b = \Delta_a' + \Delta_b'$. It is expected that the fidelity obeys $F(t) \approx 1$ within a period of time in the presence of small μ. The numerical results of $F(t)$ obtained by exact diagonalization of each invariant subspace are indicated by k.

The results for systems with representative parameters $\Delta_a + \Delta_b > 2J$ and $<2J$ are presented in Fig. 4. We can see that the results are in accord with our predictions for zero μ. We note that the fidelity experiences a sudden drop from 1 to 0 when the time reaches a boundary. For a fixed small μ, such a boundary in the time axis shrinks as the ratio Δ_a/Δ_b increases. On the other hand, for a fixed ratio Δ_a/Δ_b, such a boundary in the time axis shrinks as the μ increases. The aim of Fig. 4 is to demonstrate the continuity of the ground state when the parameter μ crosses over the zero point. The result indicates that there is no sudden change in the ground state when the parameter deviates from the fixed lines, i.e., each fixed line is not the critical line or quantum phase boundary.

VI. SUMMARY

In summary, we investigate the stability of the ground state of the p-wave Kitaev model at fixed lines in the phase diagram in the presence of a non-Hermitian pair term. Based on the exact solutions, we find that the ground state remains unchanged in the presence of a restrained non-Hermitian pair term under the periodic boundary condition for a finite system. When the translational symmetry is broken, the non-Hermitian term affects the ground state for a finite system. However, the exact solution shows that a resonant non-Hermitian impurity can induce a pair of zero modes in the corresponding Majorana lattice, which asymptotically approach the edge modes in the thermodynamic limit, manifesting the bulk-boundary correspondence. We have investigated the underlying mechanism through the equivalent quantum spin system obtained by the Jordan-Wigner transformation for finite chains. The numerical simulation of quench dynamics shows that the obtained results still hold for slight deviation from the fixed lines. In the present work we proposed a non-Hermitian Kitaev model, with the non-Hermiticity arising from locally imbalanced but globally balanced pair creation and annihilation. To date, the proposed non-Hermitian Kiteav model in the literature mainly comes from the imaginary potentials. This study provides the insight into the topological phase that emerges from the interplay between spatially separated pairing processes. In addition, the corresponding Majorana lattice of our model is non-Hermitian but possesses zero edge modes. This model can be realized in photonic systems and the edge modes can be detected in experiments [28]. Recently, it has been shown that the phase diagram of a Hermitian Kitaev model can be demonstrated in the dynamic process [29]. An interesting topic for our future work will be to investigate the dynamics of the present model.

ACKNOWLEDGMENT

This work was supported by the National Natural Science Foundation of China (under Grant No. 12374461).

APPENDIX

In this Appendix, we derive the solution of the Hamiltonian $H = H_0 + H_\pi + \sum_{k\in(0,\pi)}\psi_k^\dagger h_k \psi_k$ with zero μ, where

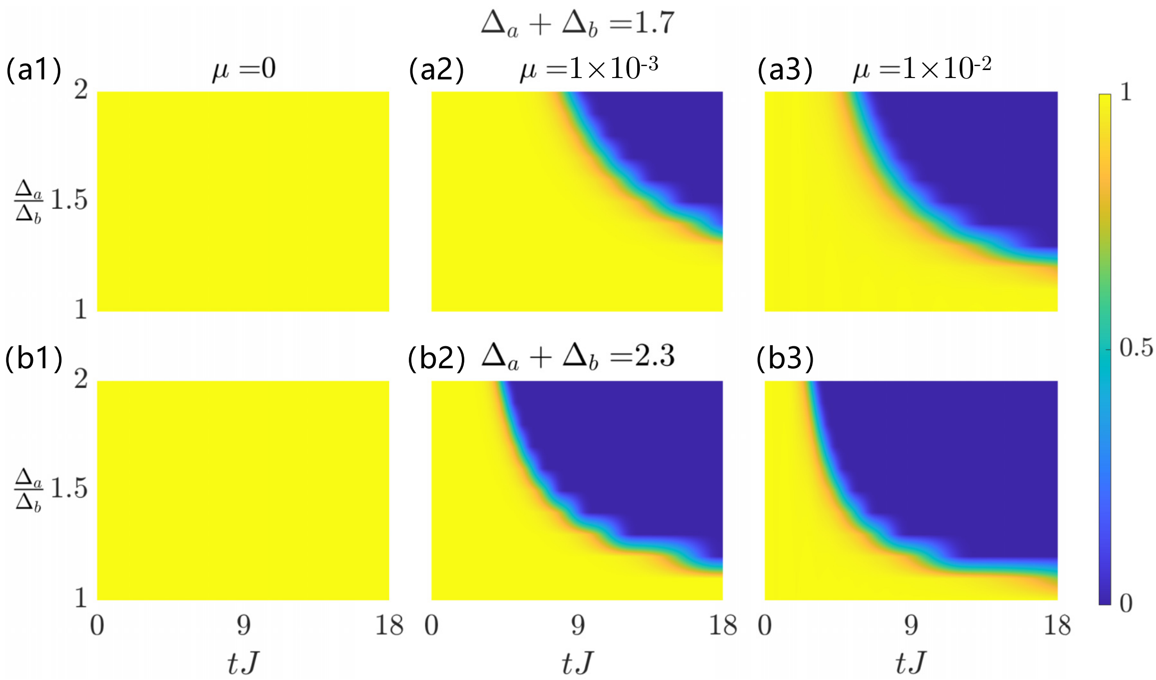

FIG. 4. 2D color contour plots of the fidelity in Eq. (43) for the quench processes. The system parameters Δ_a/Δ_b and μ are indicated in the panels. The unitary fidelity in (a1) and (b1) demonstrates our exact results. Panels (a2), (a3) and (b2), (b3) are the cases with two different values of small μ. The deep shadows indicate the region of zero fidelity. The sharp edge indicates the sudden drops of the fidelity.

$\psi_k^\dagger = (\alpha_k^\dagger \quad \beta_k^\dagger \quad \alpha_{-k} \quad \beta_{-k})$ and the core matrix h_k can be rewritten in the form

$$h_k = J\Gamma_1 + \frac{\Delta_a + \Delta_b}{2}\Gamma_2 + \frac{\Delta_a - \Delta_b}{2}\Gamma_3. \tag{A1}$$

Here, matrices

$$\Gamma_1 = \Gamma_1^\dagger = \begin{pmatrix} 0 & \gamma_{-k} & 0 & 0 \\ \gamma_k & 0 & 0 & 0 \\ 0 & 0 & 0 & -\gamma_{-k} \\ 0 & 0 & -\gamma_k & 0 \end{pmatrix} \tag{A2}$$

and

$$\Gamma_2 = \Gamma_2^\dagger = \begin{pmatrix} 0 & 0 & 0 & \gamma_{\pi-k} \\ 0 & 0 & -\gamma_{\pi+k} & 0 \\ 0 & -\gamma_{\pi-k} & 0 & 0 \\ \gamma_{\pi+k} & 0 & 0 & 0 \end{pmatrix}, \tag{A3}$$

while

$$\Gamma_3 = -\Gamma_3^\dagger = \begin{pmatrix} 0 & 0 & 0 & -\gamma_{-k} \\ 0 & 0 & \gamma_k & 0 \\ 0 & -\gamma_{-k} & 0 & 0 \\ \gamma_k & 0 & 0 & 0 \end{pmatrix} \tag{A4}$$

is anti-Hermitian with $\gamma_k = 1 + e^{ik}$. Obviously, we have

$$[h_k(\Delta_a, \Delta_b)]^\dagger = h_k(\Delta_b, \Delta_a). \tag{A5}$$

Direct derivation shows that

$$H_k = \sum_{\rho\sigma} \varepsilon_{\rho\sigma}^k \overline{A}_{\rho\sigma}^k A_{\rho\sigma}^k, \tag{A6}$$

for $k \in (0, \pi)$, where

$$\begin{aligned} A_{\rho\sigma}^k = \frac{1}{\sqrt{\Omega}}[&(1 + \rho\sigma i\, e^{(i\theta - k/2)})\alpha_k \\ &+ (\rho\, e^{i(\theta-k)} + i\sigma\, e^{-ik/2})\beta_k \\ &+ (1 - \rho\sigma i\, e^{i(\theta-k/2)})\alpha_{-k}^\dagger \\ &+ (-\rho\, e^{i(\theta-k)} + i\sigma\, e^{-ik/2})\beta_{-k}^\dagger] \end{aligned} \tag{A7}$$

and

$$\overline{A}_{\rho\sigma}^k = \left(A_{\rho\sigma}^k\right)^\dagger(\rho \to -\rho, \sigma \to -\sigma), \tag{A8}$$

with

$$\tan\theta = \frac{\sin k(2J - \Delta_a - \Delta_b)}{2J + \Delta_a + \Delta_b + \cos k(2J - \Delta_a - \Delta_b)} \tag{A9}$$

and $\sqrt{\Omega}$ being the normalization factors. The spectrum is

$$\begin{aligned} \varepsilon_{\rho\sigma}^k = \rho\sqrt{\left(2J\,\cos\frac{k}{2}\right)^2 + (\Delta_a + \Delta_b)^2\sin^2\frac{k}{2}} \\ + i\sigma(\Delta_a - \Delta_b)\cos\frac{k}{2}. \end{aligned} \tag{A10}$$

The Hamiltonian H_k is diagonalized since the set of operators $(\overline{A}_{\rho\sigma}^k, A_{\rho\sigma}^k)$ satisfies the canonical commutation relations

$$\begin{aligned} \{A_{\rho\sigma}^k, \overline{A}_{\rho'\sigma'}^{k'}\} &= \delta_{kk'}\delta_{\rho\rho'}\delta_{\sigma\sigma'}, \\ \{A_{\rho\sigma}^k, A_{\rho'\sigma'}^{k'}\} &= \{\overline{A}_{\rho\sigma}^k, \overline{A}_{\rho'\sigma'}^{k'}\} = 0. \end{aligned} \tag{A11}$$

Notably, we have

$$\begin{aligned} A^k_{\rho\sigma}A^k_{\rho\overline{\sigma}} &= \left(\overline{A}^k_{\rho\overline{\sigma}}\overline{A}^k_{\rho\sigma}\right)^\dagger \\ &= \frac{1}{\Omega}[2\rho\, e^{i\theta}(e^{-ik}\beta^\dagger_{-k}\beta_k - \alpha^\dagger_{-k}\alpha_k) \\ &\quad + (1 - e^{i(2\theta-k)})(\beta_k\alpha_k + \beta^\dagger_{-k}\alpha^\dagger_{-k}) \\ &\quad + (e^{i(2\theta-k)} + 1)(\beta^\dagger_{-k}\alpha_k + \beta_k\alpha^\dagger_{-k})] \end{aligned} \tag{A12}$$

and

$$\varepsilon^k_{\rho\sigma} + \varepsilon^k_{\rho\overline{\sigma}} = 2\,\mathrm{Re}\varepsilon^k_{\rho\sigma}, \tag{A13}$$

which are independent of $\Delta_b - \Delta_a$, with $\overline{\sigma} = -\sigma$. It indicates that any pair eigenstate in the form

$$|\psi_{\text{pair}}\rangle = \overline{A}^k_{\rho\sigma}\overline{A}^k_{\rho\overline{\sigma}}|\text{Vac}\rangle \tag{A14}$$

is independent of $\Delta_b - \Delta_a$ and has real energy

$$E_{\text{pair}} = 2\sum_{\{k\}}\mathrm{Re}\varepsilon^k_{\rho\sigma}. \tag{A15}$$

Here $|\text{Vac}\rangle$ is the vacuum state of the set of operators $\{A^k_{\rho\sigma}\}$, i.e., $A^k_{\rho\sigma}|\text{Vac}\rangle = 0$. On the other hand, the ground state of $H_0 + H_\pi$, with

$$\begin{aligned} H_0 &= 2J\alpha^\dagger_0\beta_0 + 2J\beta^\dagger_0\alpha_0 \\ &\quad + (\Delta_b - \Delta_a)(\alpha^\dagger_0\beta^\dagger_0 + \alpha_0\beta_0), \\ H_\pi &= (\Delta_b + \Delta_a)(\alpha^\dagger_\pi\beta^\dagger_\pi + \beta_\pi\alpha_\pi), \end{aligned} \tag{A16}$$

can be easily obtained by diagonalization, yielding

$$(H_0 + H_\pi)|\text{g}\rangle = -(2J + \Delta_a + \Delta_b)|\text{g}\rangle, \tag{A17}$$

with

$$|\text{g}\rangle = \tfrac{1}{2}(\alpha^\dagger_\pi\beta^\dagger_\pi + 1)(\alpha^\dagger_0 - \beta^\dagger_0)|0\rangle, \tag{A18}$$

where $|0\rangle$ is the vacuum state of the fermion operators. Obviously, the ground state is enclosed in the set of eigenstates in the form $|\psi_{\text{pair}}\rangle|\,\text{g}\rangle$.

[1] C. M. Bender and S. Boettcher, Real Spectra in Non-Hermitian Hamiltonians Having $\mathcal{PT}$ Symmetry, Phys. Rev. Lett. **80**, 5243 (1998).

[2] C. M. Bender, D. C. Brody, and H. F. Jones, Complex Extension of Quantum Mechanics, Phys. Rev. Lett. **89**, 270401 (2002).

[3] C. M. Bender, J. Brod, A. Refig, and M. E. Reuter, The C operator in $\mathcal{PT}$-symmetric quantum theories, J. Phys. A: Math. Gen. **37**, 10139 (2004).

[4] C. M. Bender, Making sense of non-Hermitian Hamiltonians, Rep. Prog. Phys. **70**, 947 (2007).

[5] D. A. McQuarrie, *Quantum Chemistry* (University Science Books, Mill Valley, CA, 1983).

[6] A. Mostafazadeh, Pseudo-Hermiticity versus $\mathcal{PT}$-symmetry: Equivalence of pseudo-Hermiticity and the presence of antilinear symmetries, J. Math. Phys. **43**, 205 (2002).

[7] A. Mostafazadeh, Pseudo-Hermiticity versus $\mathcal{PT}$-symmetry II: Equivalence of pseudo-Hermiticity and the presence of antilinear symmetries, J. Math. Phys. **43**, 2814 (2002).

[8] A. Mostafazadeh, Pseudo-Hermiticity versus $\mathcal{PT}$-symmetry III: Equivalence of pseudo-Hermiticity and the presence of antilinear symmetries, J. Math. Phys. **43**, 3944 (2002).

[9] A. Mostafazadeh, Pseudo-supersymmetric quantum mechanics and isospectral pseudo-Hermitian Hamiltonians, Nucl. Phys. B **640**, 419 (2002).

[10] A. Mostafazadeh, Pseudo-Hermiticity and generalized $\mathcal{PT}$- and $\mathcal{CPT}$-symmetries, J. Math. Phys. **44**, 974 (2003).

[11] D. Mondal and T. Nag, Anomaly in the dynamical quantum phase transition in a non-Hermitian system with extended gapless phases, Phys. Rev. B **106**, 054308 (2022).

[12] L. Jin and Z. Song, Solutions of $\mathcal{PT}$-symmetric tight-binding chain and its equivalent Hermitian counterpart, Phys. Rev. A **80**, 052107 (2009).

[13] L. Jin and Z. Song, Physics counterpart of the $\mathcal{PT}$ non-Hermitian tight-binding chain, Phys. Rev. A **81**, 032109 (2010).

[14] L. Jin and Z. Song, A physical interpretation for the non-Hermitian Hamiltonian, J. Phys. A: Math. Theor. **44**, 375304 (2011).

[15] A. Y. Kitaev, Unpaired Majorana fermions in quantum wires, Phys. Usp. **44**, 131 (2001).

[16] Y. B. Shi and Z. Song, Topological phase in a Kitaev chain with spatially separated pairing processes, Phys. Rev. B **107**, 125110 (2023).

[17] C. Nayak, S. H. Simon, A. Stern, M. Freedman, and S. D. Sarma, Non-Abelian anyons and topological quantum computation, Rev. Mod. Phys. **80**, 1083 (2008).

[18] A. Stern, Non-Abelian states of matter, Nature (London) **464**, 187 (2010).

[19] J. Alicea, New directions in the pursuit of Majorana fermions in solid state systems, Rep. Prog. Phys. **75**, 076501 (2012).

[20] S. Sachdev, *Quantum Phase Transitions* (Cambridge University Press, Cambridge, England, 1999).

[21] P. Pfeuty, The one-dimensional Ising model with a transverse field, Ann. Phys. (NY) **57**, 79 (1970).

[22] X. Z. Zhang and Z. Song, Non-Hermitian anisotropic XY model with intrinsic rotation-time-reversal symmetry, Phys. Rev. A **87**, 012114 (2013).

[23] C. Li, G. Zhang, X. Z. Zhang, and Z. Song, Conventional quantum phase transition driven by a complex parameter in a non-Hermitian $\mathcal{PT}$-symmetric Ising model, Phys. Rev. A **90**, 012103 (2014).

[24] C. Li, G. Zhang, and Z. Song, Chern number in Ising models with spatially modulated real and complex fields, Phys. Rev. A **94**, 052113 (2016).

[25] D. M. Greenberger, M. A. Horne, and A. Zeilinger, Going beyond Bell's theorem, in *Quantum Theory, and Conceptions of the Universe*, edited by M. Kafatos (Kluwer, Dordrecht, 1989), pp. 69–72.

[26] D. Bouwmeester, J.-W. Pan, M. Daniell, H. Weinfurter, and A. Zeilinger, Phys. Rev. Lett. **82**, 1345 (1999).

[27] J.-W. Pan, D. Bouwmeester, M. Daniell, H. Weinfurter, and A. Zeilinger, Experimental test of quantum nonlocality in three-photon Greenberger-Horne-Zeilinger entanglement, Nature (London) **403**, 515 (2000).

[28] S. Weimann, M. Kremer, Y. Plotnik, Y. Lumer, S. Nolte, K. G. Makris, M. Segev, M. C. Rechtsman, and A. Szameit, Topologically protected bound states in photonic parity-time-symmetric crystals, Nat. Mater. **16**, 433 (2017).

[29] Y. B. Shi, K. L. Zhang, and Z. Song, Dynamic generation of nonequilibrium superconducting states in a Kitaev chain, Phys. Rev. B **106**, 184505 (2022).